



Hesaplamalı Akışkanlar Dinamiği Yöntemi Kullanarak Üç Kanatlı Helisel Savonius Rüzgâr Türbinlerinin Aerodinamik Performansına Faz Açısı Etkisinin Araştırılması

Mernuş GÜL¹ , Muhammed Safa KAMER² , Erdem ALIÇ^{3*} 

¹Türk Havacılık ve Uzay Sanayii A.Ş., Ankara, Türkiye.

²Makine Mühendisliği Bölümü, Mühendislik Mimarlık Fakültesi, Kahramanmaraş Sütçü İmam Üniversitesi, Kahramanmaraş, Türkiye.

³Andırın Meslek Yüksekokulu, Kahramanmaraş Sütçü İmam Üniversitesi, Kahramanmaraş, Türkiye.
¹mernusdertlii@gmail.com, ²msafakamer@ksu.edu.tr, ³ealic@ksu.edu.tr

Geliş Tarihi: 03.01.2024
Kabul Tarihi: 12.02.2024

Düzeltilme Tarihi: 09.02.2024

doi: 10.62520/fujece.1414345
Araştırma Makalesi

Alıntı: M. Gül, M. S. Kamer ve E. Alıç, "Hesaplamalı akışkanlar dinamiği yöntemi kullanarak üç kanatlı helisel savonius rüzgâr türbinlerinin aerodinamik performansına faz açısı etkisinin araştırılması", *Firat Univ. Jour. of Exper. and Comp. Eng.*, vol. 3, no 1, pp. 52-64, Şubat 2024.

Öz

Bu çalışmada dikey eksenli rüzgâr türbinlerinden üç kanatlı çift kademeli helisel Savonius rüzgâr türbinlerinin (HSRT) kademeler arasındaki yarı dairesel kanatların birbirlerine olan faz açısının aerodinamik performansına olan etkisi hesaplamalı akışkanlar dinamiği (HAD) yöntemiyle incelenmiştir. Savonius rüzgâr türbini sisteminde aerodinamik performans en ciddi katkıyı sürüklenme kuvveti etkisi sağlar. Sürüklenme kuvvetine etki edebilecek performans iyileştirmeleri önemli avantajlar sağlayabilir. Bu amaç için merkezden kaçıklığı $L/H=1/2$ olan ve kademeler arasındaki yarı dairesel kanatların faz açıları $\Theta=0^\circ$, 45° ve 90° olan üç kanatlı çift kademeli helisel Savonius rotorları tasarlanmıştır. Tasarımlar için Solidworks R2018, analizler için ANSYS-Fluent 18.1 programları kullanılmıştır. $L/H=1/2$ ve $\Theta=90^\circ$ olan türbin 3B yazıcıda üretilmiş ve deneysel olarak test edilmiştir. Deneysel T-490 hava tüneline gerçekleştirilmiştir. Elde edilen sonuçlar sayısal analizlere referans olarak kullanılmış ve en ideal türbin modeli belirlenmeye çalışılmıştır. Sayısal analizde 3,83-20,35 m/s arasında değişen 10 farklı hava hızı kullanılmıştır. Sonuç olarak HSRT 1/2'lerde; faz açısının 0° 'den, 45° 'ye değiştirilmesi ile sürüklenme kuvvetinde %11,64 oranında artış görülmüştür. HSRT 1/2'lerde; faz açısının 0° 'den, 45° 'ye değiştirilmesi ile sürüklenme katsayısında %10,77 oranında düşüş olduğu görülmüştür. Sürüklenme kuvvetinde meydana gelen iyileşme ile HSRT veriminde gelişme olacağı değerlendirilmiştir.

Anahtar kelimeler: Aerodinamik özellikler, Faz açısı, Rüzgâr türbini, Hesaplamalı akışkanlar dinamiği, Sürüklenme kuvveti

*Yazışılan Yazar

İntihal Kontrol: Evet – Turnitin

Şikayet: fujece@firat.edu.tr

Telif Hakkı ve Lisans: Dergide yayın yapan yazarlar, CC BY-NC 4.0 kapsamında lisanslanan çalışmalarının telif hakkını saklı tutar



Investigation of The Effect of Phase Angle on The Aerodynamic Performance of Three-Bladed Helical Savonius Wind Turbines Using Computational Fluid Dynamics Method

Mernuş GÜL¹ , Muhammed Safa KAMER² , Erdem ALIÇ^{3*} 

¹Turkish Aerospace Industries, Ankara, Turkey.

²Department of Mechanical Engineering, Faculty of Engineering and Architecture, Kahramanmaraş Sutcu Imam University, Kahramanmaraş, Turkey.

³Andırın Vocational High School Department, Kahramanmaraş Sutcu Imam University, Kahramanmaraş, Turkey.

¹ mernusdertlii@gmail.com, ² msafakamer@ksu.edu.tr, ³ ealic@ksu.edu.tr

Received: 03.01.2024

Accepted: 12.02.2024

Revision: 09.02.2024

doi: 10.62520/fujece.1414345

Research Article

Citation: M. Gül, M. S. Kamer and E. Aliç, "Investigation of the effect of phase angle on the aerodynamic performance of three-bladed helical savonius wind turbines using computational fluid dynamics method", *Firat Univ. Jour. of Exper. and Comp. Eng.*, vol. 3, no 1, pp. 53-64, February 2024.

Abstract

In this study, the effect of the phase angle of the semicircular blades between the stages on the aerodynamic performance of the three-blade, double-stage helical Savonius wind turbines (HSWT), which are vertical axis wind turbines, was examined by the computational fluid dynamics (CFD) method. In the Savonius wind turbine system, the drag force effect provides the most significant contribution to aerodynamic performance. Performance improvements that can affect drag force can provide significant advantages. For this purpose, three-bladed double-stage helical Savonius rotors with eccentricity $L/H=1/2$ and phase angles of the semicircular blades between the stages $\Theta=0^\circ, 45^\circ$ and 90° were designed. Solidworks R2018 is used for designs and ANSYS-Fluent 18.1 programs are used for analysis. The turbine with $L/H=1/2$ and $\Theta=90^\circ$ was produced on a 3D printer and tested experimentally. Experiments were carried out in the T-490 air tunnel. The results obtained were used as a reference for numerical analysis and the ideal turbine model was tried to be determined. 10 different air velocities ranging between 3.83-20.35 m/s were used in the numerical analysis. As a result, an 11.64% increase in the drag force was observed by changing the phase angle from 0° to 45° in HSWT 1/2s. By changing the phase angle from 0° to 45° in HSWT 1/2s, a 10.77% rise in the drag coefficient was observed. It has been evaluated that the HSWT efficiency improved with the increment in drag force.

Keywords: Aerodynamic properties, Computational fluids Dynamics, Drag force, Numerical analysis, Phase angle, Wind turbine

*Corresponding author

1. Introduction

Nowadays, interest in sustainable and renewable energy sources has increased with the awareness of the decrease and limitation of underground resources that cause global warming and environmental pollution [1]. Savonius wind turbines are machines that use the kinetic energy of the wind to produce electricity and obtain mechanical power. Horizontal-axis wind turbines, which have a wide usage rate in the wind turbine group, are becoming increasingly common. There are many types of wind turbines. In the classification made according to rotor axes, they are classified as horizontal axis wind turbines and vertical axis wind turbines [2].

Vertical axis SWTs were first invented by Sigurd Savonius in 1924 and were patented in 1929 [3]. It is very easy to construct due to its simple structure. SWTs consist of two half-cylindrical blades placed between two horizontal disks and their centers shifted symmetrically to each other. Winds coming at a certain velocity create a positive moment on the inside of the cylinder and a negative moment on the outside of the cylinder. The magnitudes of these moments differ from each other. Since the moment of the inner part is greater than the moment of the outer part, rotational movement is achieved [4]. Reupke and Probert [5], to increase the operating efficiency of the SWT, replaced the curved parts of the turbine blades with a row of hinged blades. They obtained less flow resistance in the vanes that opened automatically under the influence of wind pressure. They determined that the blades automatically closed again when coming to the initial position and that at very low tip velocity rates, higher moments were obtained from the corrected segmented blade impellers compared to the classical SWTs.

Wenehenubun et al. [28] conducted an experimental study on the performance of SWTs regarding the number of blades. They compared the power coefficients, blade tip velocity ratios, and torques of one, two, three, four, and five-bladed Savonius rotors at certain wind speeds. Şahin [6] placed 6 and 8 guide plates around the classical SWT to improve wind turbine performance. The performance and velocity ratio of the SWT by changing the number, length, and position of the guide plate, were examined by taking into account the torque and momentum coefficients. An average of 30% increase in the power coefficient of the newly designed SWT was determined compared to the classical turbine. Liang et al. [7] systematically examined the radius ratio and coupling angle of a Combined Type (Savonius + Darrieus) rotor with low initial conditions but aiming for high aerodynamic performance. They investigated the effects of these two parameters on startup performance and efficiency with a computational fluid dynamics approach. They have conducted many numerical studies using the Reynolds-averaged Navier-Stokes equations and the $k-\epsilon$ turbulence model to obtain the static torque. Kothe et al. [8] numerically and experimentally examined the aerodynamic performance of the helical Savonius rotor model consisting of a 180° bent blade and the two-stage Savonius rotor model. As a result of the studies, static torque, dynamic torque, and power coefficients were compared. Although the helical Savonius rotor has a more complex manufacturing process than the two-stage SWT, it offers stable torque and a higher power coefficient. When $\lambda = 0.65$, the maximum power coefficient of the rotor was obtained in both cases. Saad et al. [9] investigated single, two, three-, and four-stage Savonius rotors with helical blades to increase the performance of vertical axis wind turbines and compared them with a single-stage Savonius rotor with aspect ratios ranging from 1 to 4. To determine performance parameters such as torque, power, and thrust coefficients, they developed a three-dimensional flow model using the Reynolds-averaged Navier-Stokes equations and the $k-\omega$ turbulence model. As a result of this study, they showed that the new design of the multistage rotor with helical blades significantly increased the output power. Evran and Yıldır [10] evaluated the drag and lift coefficient performances of NACA-4415 and NACA-0009 airfoils at constant wind velocity and various angles of attack. They determined the drag and lift coefficients of the airfoils in the ANSYS-Fluent environment. They adopted attack angles and airfoil types as control factors. In conclusion; By using the NACA4415 airfoil instead of the NACA0009 airfoil; They achieved a higher lift coefficient and lower drag coefficient. ANSYS program is one of the computer-aided engineering programs where analysis and simulations are made in engineering studies. Thanks to this program, effective studies such as mechanics, structural analysis, computational fluid dynamics and heat transfer can be carried out. In this study, flow and aerodynamic performance analysis was carried out by ANSYS-Fluent 18.1.

It has been observed in the literature that the effect of the position of the plate providing the stage to the Savonius turbine to the origin and the phase angle of the semicircular blades between the stages in Savonius turbines on the aerodynamic performance has not been investigated in helical Savonius turbines. In this study, unlike the literature, the effect of the plate's position providing the stage and the phase angle of the semicircular blades between the stages on the aerodynamic performance of the three-bladed, double-stage helical Savonius turbine has been a numerical investigation. The novelty of this study is to investigate the performance improvement of 3-blade HSWT by changing the phase angle. For this purpose, the aerodynamic analysis (lift and drag forces and lift and drag coefficients) of the HSWT were examined numerically.

2. Material and Method

In this study, a research CFD investigation was conducted on the three-bladed double-stage HSWT, which is a vertical axis wind turbine model. In particular, the effect of the phase angle of the semicircular blades between the stages on the aerodynamic performance was examined. The eccentricity of the model examined is $L/H=1/2$ and the phase angle is $\Theta = 0^\circ, 45^\circ, \text{ and } 90^\circ$, respectively. The rotor length of HSWT is $(H) = 110$ mm, rotor diameter $(D) = 46$ mm, and shaft diameter $(d) = 5$ mm. The designs for the effect of the phase angle on the turbine in geometries with eccentricity $L/H=1/2$ are given in Figure 1.

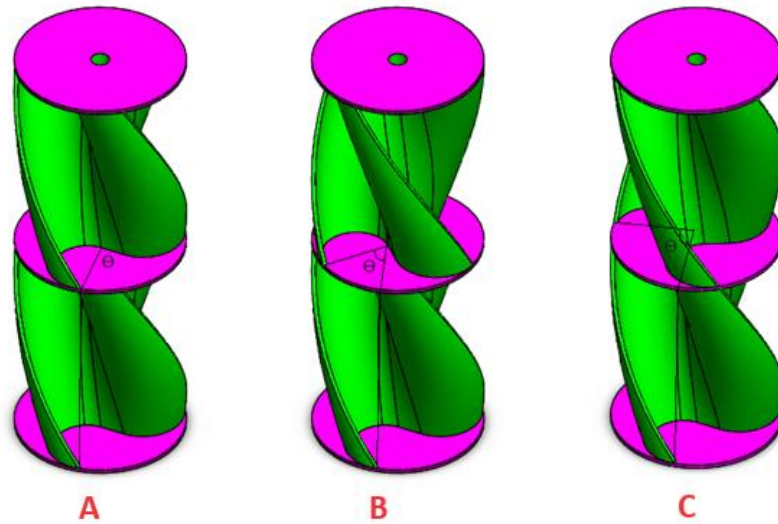


Figure 1. Design of the different phase angle HSWTs a) $\Theta = 0^\circ$, b) $\Theta = 45^\circ$, c) $\Theta = 90^\circ$

The production of the HSWT, which was designed in the Solidworks environment, with an eccentricity of $L/H = 1/2$, was carried out with an Ultimaker Extended 2 3D printer. PLA filament is used in the solid model produced for experimental studies. Considering the surface roughness and manufacturing time of the wind turbine produced; A layer thickness of 0.1 mm was determined and a 0.40 mm nozzle tip was used.

In this study, experimental studies were carried out on a wind turbine with $L/H = 1/2$ to determine the initial and boundary conditions in numerical studies. Fifty experiments were carried out with this experimental turbine at ten different air velocities, and these processes were repeated three times. Then, air velocity (V_s), number of revolutions (n), and drag force (F_d) were measured by taking average values. Reynolds number (Re), drag coefficient (C_d), and blade tip velocity ratio (λ) were calculated. The air tunnel used in the experiment is an open-air tunnel. The T-490 air tunnel is designed to conduct experiments in the fields of aerodynamics and fluid mechanics. The Savonius rotor produced by the 3D printer was placed in the test area of the experimental setup. Experiments were carried out for the turbine with $L/H = 1/2$ at 10 different air velocities in the air tunnel, and the air tunnel test area during the experiment is shown in Figure 2.



Figure 2. Air tunnel test area during the experiment

Savonius rotors work with the effect of drag force. The drag force F_d is given in Eq. 1 and the drag coefficient C_d is given in Eq. 2. In these equations, V_s is the wind velocity, A_p is the projection area, ρ is the density of the air and C is the aerodynamic coefficient [11,12].

$$F_d = \frac{1}{2} \cdot A_p \cdot C_d \cdot \rho \cdot V_s^2 \quad (1)$$

$$C_d = \frac{F_d}{\frac{1}{2} \cdot A_p \cdot \rho \cdot V_s^2} \quad (2)$$

The Reynolds number is used to determine the characteristics of different flow regimes, such as laminar flow or turbulent flow. The flow regime depends on the ratio of inertial forces to viscous forces in the fluid [13]. Reynolds number (Re) given in Eq. 3 [14].

$$Re = \frac{\rho \cdot V_s \cdot d}{\mu} \quad (3)$$

After carrying out many experiments, one of the methods developed to determine the error rates of the experiments is the "Uncertainty Analysis" method [15,16]. The uncertainty of the drag coefficient C_d in this study was calculated using Eq. 4 and Eq. 5.

$$C_d = f(F_d, V_s, A_p, \rho) \quad (4)$$

$$W_{C_d} = \left[\left(\frac{\partial C_d}{\partial F_d} \cdot W_{F_d} \right)^2 + \left(\frac{\partial C_d}{\partial V_s} \cdot W_{V_s} \right)^2 + \left(\frac{\partial C_d}{\partial A_p} \cdot W_{A_p} \right)^2 + \left(\frac{\partial C_d}{\partial \rho} \cdot W_{\rho} \right)^2 \right]^{1/2} \quad (5)$$

When the studies investigating the aerodynamic performance of SWTs are examined; In many studies, it has been determined that only the test area of the air tunnel is modeled. Similarly, in this study; Considering the analysis times and the working capacity of the workstation, the flow volume created when the wind turbine model was placed in the test chamber was modeled and the airflow was defined as linear. When the wind turbine model was placed in the 200mm x 200mm x 500mm test chamber of the air tunnel, the resulting flow volume obtained as CAD data through the SOLIDWORKS program, and a network structure defined for this geometry in the ANSYS-Fluent program. By comparing the experiments and analysis results, problems that may arise from the experimental setup or analysis investigated and the most suitable mesh for the analysis obtained. The CAD drawing and mesh of the air tunnel (test zone) are depicted in Figure 3.

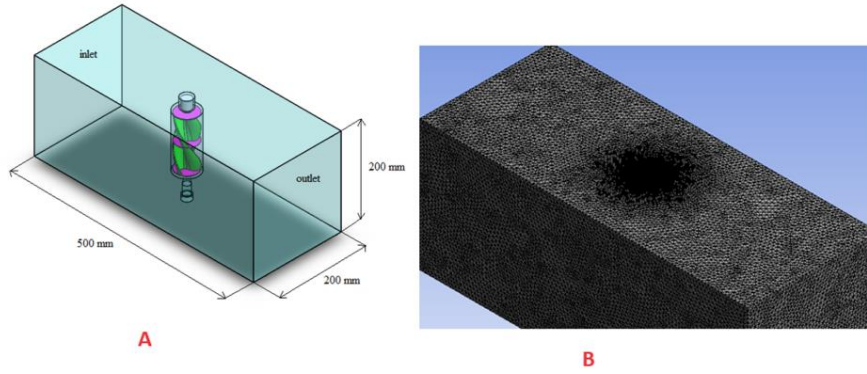


Figure 3. Air tunnel test domain a) Solid model b) Mesh model

The following values were chosen as initial and boundary conditions in the numerical analysis; Air was chosen as the fluid in the analysis carried out in the ANSYS-Fluent program. 'Velocity-inlet' is defined as the entrance section of the air to the test area (air tunnel). Air velocities are $V_s=3.83$ m/s, 6.83 m/s, 8.47 m/s, 10.15 m/s, 11.67 m/s, 13.26 m/s, 15.28 m/s, 16.76 m/s, 18.76 m/s and 20.35 m/s. In numerical studies, the $k-\epsilon$ realizable turbulence model is used as the turbulence model. Analysis was performed steady state. 'Pressure outlet' is defined as the section where the air exits the test area. Except for the parts defined as velocity-inlet and pressure-outlet, the outer regions of the test region are defined as 'wall'. For the continuity equation, a convergence condition of up to 10^{-4} was used [17]. Some grid specifications are given in Table 1.

Table 1. Grid specifications

| Body Sizing - Domain | Face Sizing - Wall | Face Sizing - Other | Body Sizing - Rotary | Face Sizing - Turbine | Skewness (max.) | Growth Rate |
|----------------------|--------------------|---------------------|----------------------|-----------------------|-----------------|-------------|
| 5mm | 5mm | 1mm | 3mm | 0.5mm | 0.88 | 1.05 |

When the studies on improving the aerodynamic performance of SWT were examined in the literature, it determined that the $k-\epsilon$ realizable turbulence model was widely used and this turbulence model gave better results. Due to the success of the $k-\epsilon$ realizable turbulence model in HSWT flow analysis, $k-\epsilon$ realizable was chosen as the turbulence model in this study. The transport equations valid for turbulent kinetic energy (k) and loss rate (ϵ) are written as given in Equation 6 and Equation 7, respectively.

Turbulence Kinetic Energy (k) equation in Eq.6 ;

$$\frac{\partial}{\partial t}(\rho k) + \frac{\partial}{\partial x_j}(\rho k u_j) = \frac{\partial}{\partial x_j} \left[\left(\mu + \frac{\mu_t}{\sigma_k} \right) \frac{\partial k}{\partial x_j} \right] + G_k + G_b - \rho \epsilon - Y_M + S_k \quad (6)$$

Loss Rate (ϵ) equation in Eq.7 ;

$$\frac{\partial}{\partial t}(\rho \epsilon) + \frac{\partial}{\partial x_j}(\rho \epsilon u_j) = \frac{\partial}{\partial x_j} \left[\left(\mu + \frac{\mu_t}{\sigma_\epsilon} \right) \frac{\partial \epsilon}{\partial x_j} \right] + \rho C_{1\epsilon} S_\epsilon - \rho C_{2\epsilon} \frac{\epsilon^2}{k + \sqrt{\vartheta \epsilon}} + C_{1\epsilon} \frac{\epsilon}{k} C_{3\epsilon} G_b + S_\epsilon \quad (7)$$

Turbulence viscosity equation in Eq.8;

$$C_1 = \max \left[0.43; \frac{\eta}{\eta + 5} \right], \quad \eta = S \frac{k}{\epsilon}, \quad S = \sqrt{2S_{ij}S_{ij}} \quad (8)$$

The constant values used in the turbulence model of this study are as follows;

$$C_{1\epsilon} = 1.44, \quad C_{2\epsilon} = 1.9, \quad \sigma_k = 1.0, \quad \sigma_\epsilon = 1.2$$

3. Result and Discussion

In this study, the effect of the phase angle between the stages of the HSWT on the aerodynamic performance was examined numerically. The drag force and drag coefficient of double-stage helical Savonius wind turbines (HSWT 1/2) with eccentricity $L/H=1/2$ were investigated at different phase angles ($\Theta=0^\circ, 45^\circ$, and 90°), and ten different air velocities. First, the grid independence study of the 3D-designed digital model was carried out. Second, experimental studies were carried out on HSWT ($L/H=1/2$) 90° to serve as a reference for numerical analysis. Moreover, the last, the experimental results were compared with all other numerical analysis results.

For mesh independence analysis, analysis was carried out with four different numbers of elements. In the analysis, the number of personnel starts from approximately 13 million and goes up to 17.5 million. Figure 4 shows the mesh independence study. Since the analysis, results were very close to each other after the number of elements was 14 million, the mesh model with the number of elements 14 million was chosen. Another reason for choosing the model with 14 million elements is that it reduces the analysis time. The results given hereafter are the same as the mesh model with 14097168 elements.

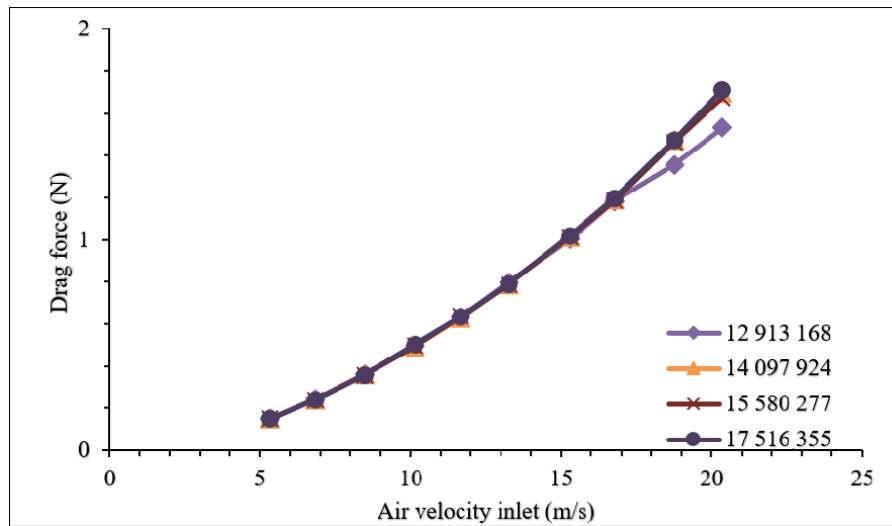


Figure 4. Domain mesh independency

ANSYS program is one of the computer-aided engineering programs where analysis and simulations are made in engineering studies. Thanks to this program, effective studies such as mechanics, structural analysis, computational fluid dynamics, and heat transfer were carried out. ANSYS is one of the most used CAE (computer-aided engineering) programs in Turkey and uses the finite element method (FEA) [18]. In the literature, the ANSYS-Fluent program is frequently used in the analysis of wind turbines [19, 20].

Experiments were carried out on HSWT1/2 90° to verify the numerical results in this study. The experimental results and the numerical analysis results are shown in Figure 5. The effect of air velocity on the drag force was examined for numerical analysis and comparison with experimental results. According to Figure 5, as the air velocity increases, the error rate of the numerical analysis also increases. Here, at the highest velocity of 20.35m/s, the maximum error rate does not exceed 15%. When 3D WT studies in the literature were examined, this error rate was considered acceptable [21–23].

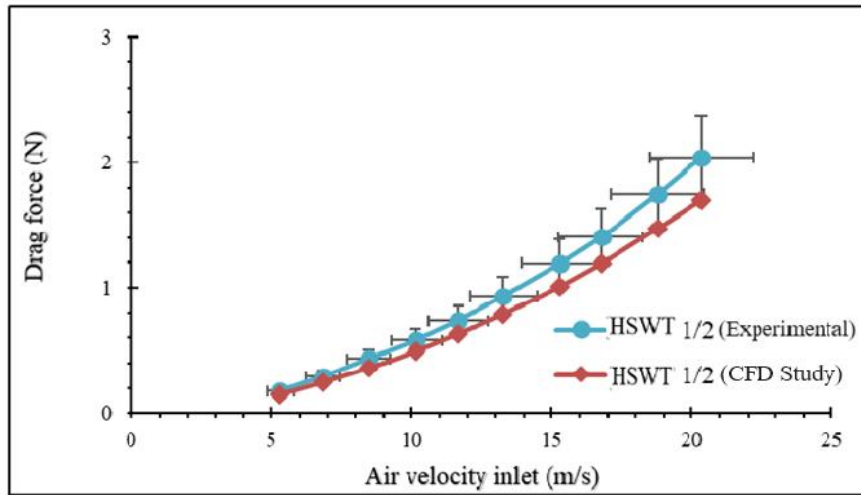


Figure 5. Domain mesh independency

In Savonius wind turbines, drag force directly affects aerodynamic performance. Many researchers have stated that as the drag force increases, the torque or power generation also increases [24–26]. Utomo et al. In their experimental studies, they stated that by adding a fin to the SWT, they obtained a drag force that increased the efficiency [27]. The effect of the phase angle between the stages of three different wind turbines on the aerodynamic performance was examined numerically. The effect of air velocity on the drag force (N) at different phase angles (Θ) of double-stage helical Savonius wind turbines (HSWT 1/2) with eccentricity $L/H=1/2$ is given in Figure 6.

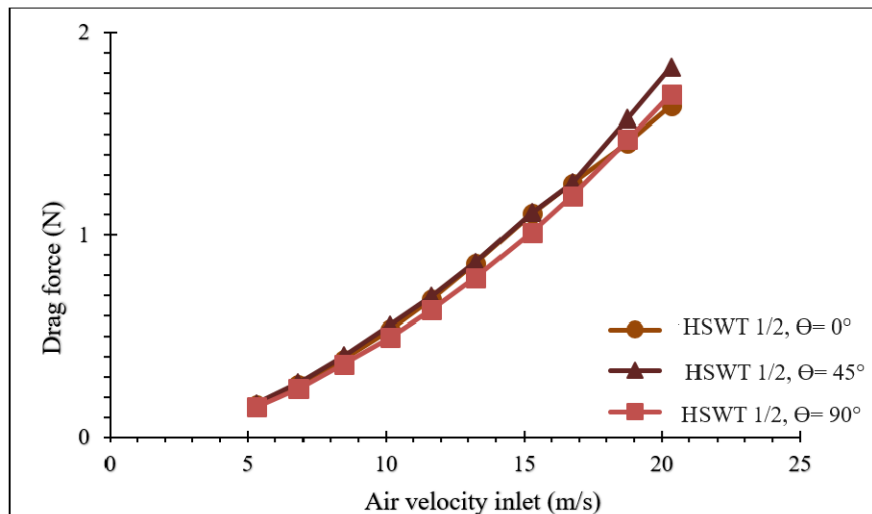


Figure 6. Effect of air velocity on drag force in HSWT 1/2s

According to Fig. 6, the drag force increased as the air velocity increased for all three geometries. When compared according to phase angles, the drag force of HSWT 1/2, $\Theta=45^\circ$ was higher than the others. As a result, for the highest air velocity (20.35 m/s) in HSWT 1/2s, An increase of 11.64% in the drag force was observed by increasing the phase angle from 0° to 45° . In HSWT 1/2s, by increasing the phase angle from 45° to 90° , a 7.24% decrease in the drag force was observed. The effect of the Reynolds number on the drag coefficient in double-stage helical Savonius wind turbines (HSWT 1/2) with eccentricity $L/H=1/2$ is given in Figure 7.

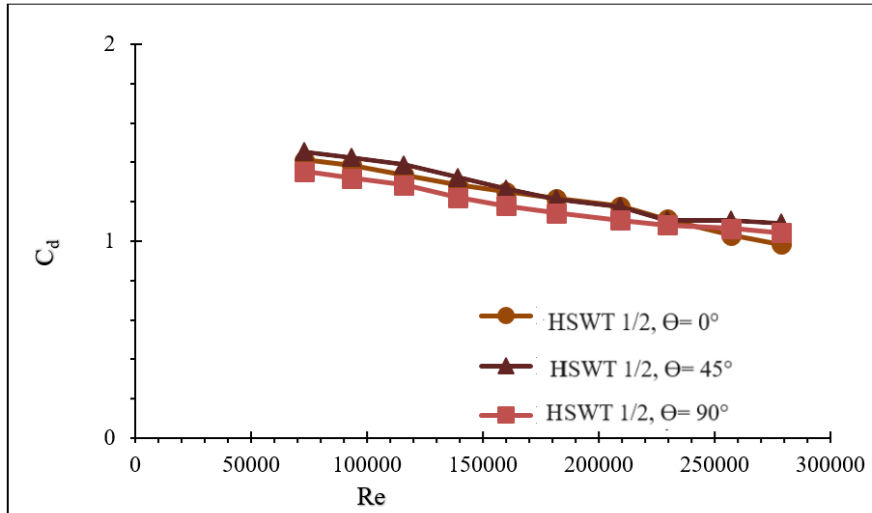


Figure 7. Effect of Reynolds number on drag coefficient in HSWT 1/2s

Wenehenubu et al. [28] studied the SWT performance related to the number of blades. They stated that the drag force of the four-bladed SWT was higher than that of the two- and three-bladed SWTs. For this reason, they stated that the four-blade SWT has produced more torque. In this study, it was tried to determine the HSWT model with the highest drag force at three different phase angles. When compared according to phase angles; It was observed that the drag coefficient of HSWT 1/2, $\Theta=45^\circ$ was higher than the others. As a result, for the highest air velocity (20.35 m/s); In HSWT1/2s, by increasing the phase angle from 0° to 45° , a 10.77% increase in the drag coefficient was observed. In HSWT 1/2s, by increasing the phase angle from 45° to 90° , a 4.29% decrease in the drag coefficient was observed. At maximum air velocity (20.35 m/s), according to numerical results, HSWT 1/2 gives the best result, $\Theta=45^\circ$; the velocity distribution in the origin section of the test area of the air tunnel is depicted in Figure 8.

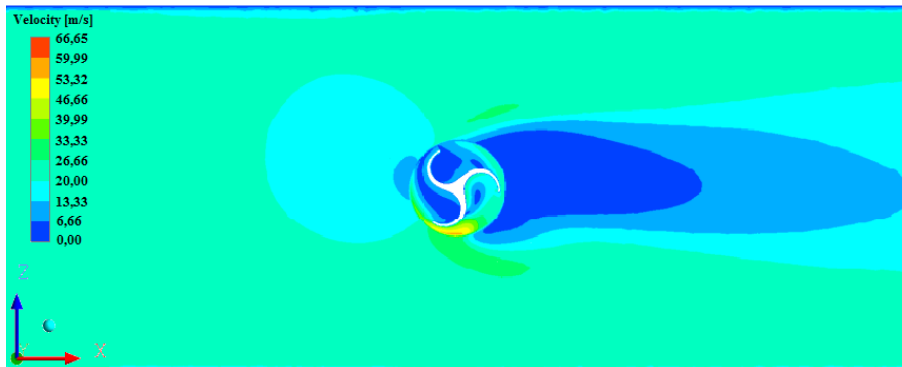


Figure 8. Velocity contour distribution created by HSWT 1/2 $\Theta=45^\circ$ in the test region (origin section)

According to Figure 8, it observed that the air velocity decreased slightly in front of the turbine, and behind the turbine, the air velocity decreased considerably and almost stopped. At maximum air velocity (20.35 m/s), HSWT 1/2 $\Theta=45^\circ$, the pressure distribution in the origin section of the test area of the air tunnel is shown in Figure 9.

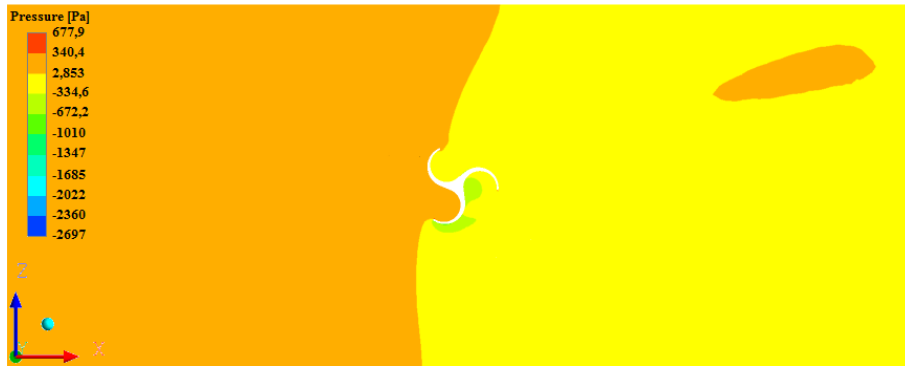


Figure 9. Pressure distribution created by HSWT 1/2 $\Theta=45^\circ$ in the test area (origin section)

Figure 10 shows that the velocity vectors progress linearly from the inlet part. The velocity vectors increase immediately around the turbine. Especially, high-velocity distribution arrows are seen in the flow region breaking away from HSWT 1/2, $f = 45^\circ$. Low-velocity distribution arrows are seen just behind the turbine. High-velocity distribution arrows are seen in the area breaking away from the lower and upper plates. The arrows scattered on the edges and behind the turbine become linear again towards the outlet section.

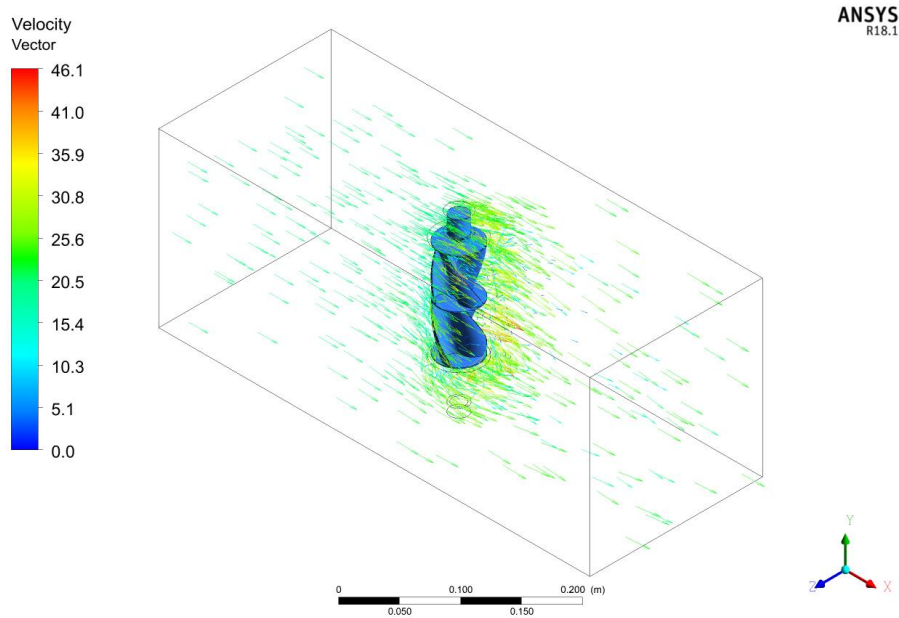


Figure 10. Velocity distribution created by HSWT 1/2 $\Theta=45^\circ$ in the test area

The optimum wind turbine geometry was tried to be obtained by examining the drag and lift forces, drag and lift coefficients, as well as the effects on the power coefficient and speed of the 3-blade HSWT at different air velocities. With this, the HSWT model with high energy efficiency has been introduced. As a result, electrical energy will be produced with less loss. It is evaluated that electrical energy produced more and at a cheaper cost will minimize the use of fossil fuels.

4. Conclusion

In this study, the aerodynamic performance of the phase angle of the semicircular blades between the stages of a three-bladed double-stage HSWT was investigated by the CFD method. The power obtained from wind turbines is determined by the lift and drag forces they have at certain wind velocities. For HSWTs to be more efficient, a good drag force must be obtained from the existing drag force.

- In HSWT 1/2s, it was observed that there was an increase of 11.64% in the drag force by changing the phase angle from 0° to 45°.
- In HSWT 1/2s, it was observed that there was a 10.77% increase in the drag coefficient by changing the phase angle from 0° to 45°.
- In HSWT 1/2s, it was observed that there was a 7.24% decrease in the drag force by changing the phase angle from 45° to 90°.

In this study, the good performance model among the HSWTs examined was determined as HSWT 1/2 $\Theta = 45^\circ$. The drag force and drag coefficient of this model are raiser than other models. In the future, new generation wind turbines will develop by combining different types of wind turbines into the ideal model determined in this study.

5. Acknowledgement

This study was supported by the KSU Scientific Research Unit (BAP Project No: 2021/2-3YLS).

6. Author Contribution Statement

Mernuş GÜL: Formation of the idea, design, numerical analysis, and literature review, M. Safa KAMER: Formation of the idea, numerical analysis, and project manager, Erdem ALIÇ: supervised the whole research work and reviewed the writing – original draft, project researcher, All authors have approved the final version.

7. Ethics Committee Approval and Statement of Conflict of Interest

There is no need to obtain ethics committee permission for the article prepared. There is no conflict of interest with any person/institution in the prepared article.

8. List of Abbreviations

A: Area, m²
Cd: Drag coefficient,-
CFD: Computational fluids Dynamics
Fd: Drag force, N
HSWT: Helical Savonius wind turbine
k: Turbulent kinetic energy, J/kg
Re: Reynolds number
SWT: Savonius wind turbine
Vs: airflow velocity, m/s
WT: Wind turbine
 Θ : Phase angle
 ρ : Air density, kg/m³
3D: Three dimension

9. References

- [1] K. K. Jaiswal, C. R. Chowdhury, D. Yadav, R. Verma, S. Dutta, K. S. Jaiswal, SangmeshB and K. S. K. Karuppasamy, “Renewable and sustainable clean energy development and impact on social, economic, and environmental health”, *Ener. Nex.*, vol. 7, pp. 100118, April 2022.
- [2] M. Pourhoseinian, S. Sharifian and N. Asasian-Kolur, “Unsteady-state numerical analysis of advanced Savonius wind turbine”, *Energy Sources, Part A Recover. Util. Environ. Eff.*, vol. 00, no. 00, pp. 1–16, 2021.
- [3] D. Afungchui, B. Kamoun, A. Helali and A. Ben Djemaa, “The unsteady pressure field and the aerodynamic performances of a Savonius rotor based on the discrete vortex method,” *Renew. Energy*, vol. 35, no. 1, pp. 307–313, 2010.
- [4] T. Ogawa, “Theoretical study on the flow about savonius rotor,” *J. Fluids Eng. Trans. ASME*, vol. 106, no. 1, pp. 85–91, 1984.
- [5] P. Reupke and S. D. Probert, “Slatted-blade Savonius wind-rotors,” *Appl. Energy*, vol. 40, no. 1, pp. 65–75, 1991.
- [6] İ. Şahin, “Bir savonius rüzgar türbininin performansının sayısal incelenmesi ve iyileştirilmesi, Gazi Üniversitesi,” *Fen Bilim. Enstitüsü Enerj. Sist. Mühendisliği, Yüksek Lisans Tezi*, 2015.
- [7] X. Liang, S. Fu, B. Ou, C. Wu, C. Y. H. Chao and K. Pi, “A computational study of the effects of the radius ratio and attachment angle on the performance of a Darrieus-Savonius combined wind turbine”, *Renew. Energy*, vol. 113, pp. 329–334, 2017.
- [8] L. B. Kothe, S. V. Möller and A. P. Petry, “Numerical and experimental study of a helical Savonius wind turbine and a comparison with a two-stage Savonius turbine”, *Renew. Energy*, vol. 148, pp. 627–638, 2020.
- [9] A. S. Saad, A. Elwardany, I. I. El-Sharkawy, S. Ookawara and M. Ahmed, “Performance evaluation of a novel vertical axis wind turbine using twisted blades in multi-stage Savonius rotors”, *Energy Convers. Manag.*, vol. 235, no. February, p. 114013, 2021.
- [10] S. Evran and S. Z. Yildir, “Numerical and statistical aerodynamic performance analysis of NACA0009 and NACA4415 airfoils”, *J. Polytech.*, vol. 0900, pp. 0–2, 2023.
- [11] B. Deda Altan and G. S. Gultekin, “Investigation of performance enhancements of savonius wind turbines through additional designs,” *Processes*, vol. 11, no. 5, 2023.
- [12] M. Basumatary, A. Biswas and R. D. Misra, “CFD study of a combined lift and drag-based novel Savonius vertical axis water turbine”, *J. Mar. Sci. Technol.*, vol. 28, no. 1, pp. 27–43, 2023.
- [13] Y. A. Cengel and A. J. Ghajar, “Heat and mass transfer (a practical approach, SI version)”, McGraw-Hill Education, 2011.
- [14] Y. A. Çengel and J. M. Cimbala, “Fluid Mechanics: Fundamentals and Applications, Forth Edition”, New York: McGraw-Hill Education, 2018.
- [15] T. S. Rengma and P. M. V. Subbarao, “Optimization of semicircular blade profile of Savonius hydrokinetic turbine using artificial neural network”, *Renew. Energy*, vol. 200, no. September, pp. 658–673, 2022.
- [16] M. Basumatary, A. Biswas and R. D. Misra, “Experimental verification of improved performance of Savonius turbine with a combined lift and drag based blade profile for ultra-low head river application”, *Sustain. Energy Technol. Assessments*, vol. 44, no. December 2020, p. 100999, 2021.
- [17] K. R. Abdelaziz, M. A. A. Nawar, A. Ramadan, Y. A. Attai and M. H. Mohamed, “Performance investigation of a Savonius rotor by varying the blade arc angles”, *Ocean Eng.*, vol. 260, no. July, p. 112054, 2022.
- [18] A. Fluent, “ANSYS fluent theory guide 15.0,” ANSYS, Canonsburg, PA, 2013.
- [19] A. Hesami, A. H. Nikseresht and M. H. Mohamed, “Feasibility study of twin-rotor Savonius wind turbine incorporated with a wind-lens”, *Ocean Eng.*, vol. 247, no. January, p. 110654, 2022.
- [20] H. E. Tanürün, İ. Ata, M. E. Canlı and A. Acir, “Farklı açıklık oranlarındaki NACA-0018 rüzgâr türbini kanat modeli performansının sayısal ve deneysel incelenmesi”, *Politek. Derg.*, vol. 23, no. 2, pp. 371–381, 2020.
- [21] D. H. Didane, M. N. A. Bajuri, M. I. Boukhari and B. Manshoor, “Performance investigation of vertical axis wind turbine with savonius rotor using computational fluid dynamics (CFD)”, *CFD Lett.*, vol. 14, no. 8, pp. 116–124, 2022.

- [22] H. A. Hassan Saeed, A. M. Nagib Elmekawy and S. Z. Kassab, “Numerical study of improving Savonius turbine power coefficient by various blade shapes”, *Alexandria Eng. J.*, vol. 58, no. 2, pp. 429–441, 2019.
- [23] M. S. Abdullah, M. H. H. Ishak and F. Ismail, “Numerical study of the 3D Savonius turbine under stationary conditions”, *Eng. Fail. Anal.*, vol. 136, no. February, p. 106199, 2022.
- [24] M. H. M. Al Ghriyah, “An experimental study on improvement of a savonius rotor performance with multiple halves blades”, Near East University, 2017.
- [25] M. M. Kamal and R. P. Saini, “A numerical investigation on the influence of savonius blade helicity on the performance characteristics of hybrid cross-flow hydrokinetic turbine”, *Renew. Energy*, vol. 190, pp. 788–804, 2022.
- [26] M. B. Salleh, N. M. Kamaruddin and Z. Mohamed-Kassim, “The effects of deflector longitudinal position and height on the power performance of a conventional Savonius turbine”, *Energy Convers. Manag.*, vol. 226, no. August, p. 113584, 2020.
- [27] I. S. Utomo, D. D. D. P. Tjahjana and S. Hadi, “Experimental studies of Savonius wind turbines with variations sizes and fin numbers towards performance”, *AIP Conf. Proc.*, vol. 1931, 2018.
- [28] F. Wenehenubun, A. Saputra and H. Sutanto, “An experimental study on the performance of Savonius wind turbines related with the number of blades”, *Energy Procedia*, vol. 68, pp. 297–304, 2015.